Journal of Inorganic and General Chemistry
ZAAC
Zeitschrift für anorganische und allgemeine Chemie
www.zaac.wiley-vch.de
RESEARCH ARTICLE

DOI: 10.1002/zaac.202500046

Flux Growth of La_3MC_2 (M = Sb, Bi, Te), a New Family of Ternary Carbides

Luke Marzano, Mohammed Sahab Uddin, Amirhossein Zareihassangheshlaghi, Olufemi Araoyinbo, Juan Hernandez, and Susan Latturner*

This article dedicated to Professor Gordon Miller on the occasion of his 65th birthday

Reactions of carbon with a heavy main group metal (M = Sb, Bi, or Te) in an excess of lanthanum/nickel eutectic flux lead to formation of a family of carbide compounds La_3MC_2 with a new structure type. The monoclinic structure features C_2^{4-} anions octahedrally coordinated by six La^{3+} cations, and M anions surrounded by 8 La^{3+} cations. These compounds are not charge-balanced and lie on the border between intermetallic carbides and mixed anion salts. Density of states calculations show a pseudogap at the Fermi level for La_3BiC_2, which indicates that this compound is a poor metal with optimized La—Bi bonding interactions.

1. Introduction

Ternary lanthanide carbide compounds are of interest due to the complex structures and mixtures of bonding types that can occur due to the combination of covalent bonds to carbon, ionic interactions between lanthanide cations and carbide anions, and metallic bonding throughout the lanthanide framework. Ternary $Ln_xT_yC_z$ compounds (with T = transition metal) are divided into metal-rich carbides and carbometallates.[1] Metal-rich carbides feature interstitial carbon atoms surrounded by a metallic network of transition metal and lanthanide ions, exemplified by the strongly magnetic compounds $Nd_2Fe_{14}C$ and $Sm_2Fe_{17}C_2$.[2,3] Carbometallates such as $La_{11}(MnC_6)_3$ and $Pr_{14}Fe_6C_{13}$ are more carbon-rich and contain covalent T—C clusters or chains, surrounded by Ln cations.[4,5] Ternary $Ln_xX_yC_z$ (with X = halides) compounds are often charge-balanced, with the X^- and C_2^{n-} anions surrounded by lanthanide cations. This class of materials includes the superconducting compounds $La_2X_2C_2$ (X = Br, I).[6,7] The prevalence of superconductivity in binary, ternary, and quaternary lanthanide carbides was highlighted by Miller in 1996.[8] Kremer, Kim, and Simon presented an overview of the electronic structures of superconducting $Ln_2X_2C_2$ in 2007.[9] Both works indicate the importance of the C_2 unit and the location of its states with respect to the Fermi level of these materials.

Reviews of literature on ternary lanthanide carbides indicate that, while a plethora of $Ln_xT_yC_z$ and $Ln_xX_yC_z$ compounds exist and they have been heavily explored, less is known about Ln/M/C ternary compounds with M = main group metal.[10–12] There are several distinct gaps in existing $Ln_xM_yC_z$ phases.[12] For instance, aside from $Ln_6Mg_{23}C$, there are no reported lanthanide alkaline earth carbides. There is also a lack of ternary compounds with M = heavy pnictides and chalcogenides. This may be due to the preferred formation of stable binary compounds such as La_5Bi_3, LaBi, and La_2Te_3, as well as the relative inertness of carbon compared to the M element. Formation of simple binary phases can be avoided by using metal flux synthesis, which enables lower reaction temperatures and brings all the reactants into solution.[13] This minimizes the problems of different element melting points, reactivities, and diffusion rates, which can lead to their segregation into different products.

In this work, we used lanthanum/nickel eutectic as a flux. The 75 mol% La: 25 mol% Ni eutectic ratio melts at 520 °C and has been shown to be an excellent solvent for carbon and a fruitful medium for crystal growth of new complex carbides such as $La_{11}(MnC_6)_3$ and $La_{21}Fe_8Sn_7C_{12}$.[4,14] The reaction of carbon with M = Sb, Bi, or Te in La/Ni flux has yielded a new family of La_3MC_2 compounds containing the C_2 anion as well as M anions. These two anions are each surrounded by La^{3+} cations in the structure. While these materials might be assumed to be saltlike, density of states (DOS) calculations show that they are not charge-balanced and are poor metals. Formation of analogs with different M elements shows that this structure can form with a variable range of valence electron count.

2. Experimental Section

2.1. Synthesis

A lanthanum/nickel eutectic mixture was used as the flux for these reactions. To prepare the eutectic, pieces of La metal (Beantown Chemical, 99.9%), and nickel slugs (Beantown Chemical, 99.95%) were weighed out in a 88:12 mass ratio. These pieces were placed together in a hollow on a copper-cooled hearth within an arc-melter chamber. The elements were then arc-melted together under argon. The resulting button was

L. Marzano, M. S. Uddin, A. Zareihassangheshlaghi, O. Araoyinbo, J. Hernandez, S. Latturner
Department of Chemistry, Florida State University, Tallahassee, FL 32306, USA
E-mail: slatturner@fsu.edu

flipped and remelted several times to ensure homogeneity. After cooling down, it was broken into pieces to be used as a flux.

For the synthesis of each La_3MC_2 analog, 1.5 g of the La/Ni eutectic were placed in an alumina crucible along with 1 mmol of carbon (acetylene carbon black, Strem Chemicals, 99.99%) and 0.5 mmol of the *M* element (Sb powder from Strem Chemicals at 99.5% purity, Bi powder from Alfa Aesar at 99.5%, or Te powder from Ventron at 99.99% purity). The crucibles were then placed in fused silica tubes with a wad of silica wool above the crucible to act as a filter. The tubes were attached to a vacuum line and then flame-sealed under a pressure below 100 mTorr. These ampules were then placed in a furnace and heated to 1000 °C in 5 h, held at this temperature for 12 h, and then cooled down to 625 °C in 96 h. The ampules were removed from the furnace at this temperature, inverted, and centrifuged to remove the remaining molten flux from the products. The ampules were cracked open and the product crystals removed and stored under nitrogen. The title phase crystals are air sensitive and moisture sensitive but can be handled briefly in air.

2.2. Elemental Analysis

Crystals of each compound were selected using an optical microscope and mounted on an aluminum sample puck using carbon tape, positioning the crystals so a clean flat surface was faced upward. Elemental analysis was performed using an FEI NOVA 400 scanning electron microscope equipped with energy-dispersive X-ray spectroscopy (SEM–EDS). An acceleration voltage of 20 kV was used for the EDS measurements. While carbon peaks were observed, quantification was not possible due to the limitation of this technique with light elements and the background from the use of carbon tape. Carbon content was instead determined by the crystal structure refinement (see next section). Atomic percentages of metal elements were averaged over several samples, avoiding sampling surfaces that were coated with flux residue. The average La:M atomic percentage values were 75.9(8)%:24.1(8)% for all three La_3MC_2 compounds, in agreement with the 3:1 composition indicated by the structure determination. No indications of incorporation of nickel from the flux or aluminum from the crucible were observed.

2.3. Crystallographic Studies

Small single crystal samples of each analog were cleaved from larger crystals under an optical microscope. These were mounted on a cryoloop using Parabar oil. Single-crystal X-ray diffraction data were collected using a Rigaku XtaLAB Synergy-S diffractometer equipped with a HyPix-6000HE hybrid-photon counting detector and Mo/Cu microfocus-sealed X-ray sources. The programs CrysalisPro and Shelxle were used to process the data and refine the structure.[15,16] All of the analogs were solved in monoclinic space group $P2_1/m$. Lanthanum and *M* atom sites were located using direct methods; the carbon site was found via analysis of residual electron density peaks. After all peaks were assigned to atoms, the only remaining electron density peaks were small artifacts close to heavy atoms (less than 1 Å from La or Bi). Crystallographic data and collection parameters are shown in **Table 1**. Further details of the crystal structure investigations may be obtained from the Fachinformationzentrum Karlsruhe, D-76 344 Eggenstein-Leopoldshafen, Germany, on

Table 1. Crystallographic data and collection parameters for the title compounds.

Formula	La_3SbC_2	La_3BiC_2	La_3TeC_2
Formula weight [g mol^{-1}]	562.51	649.73	568.35
Crystal System		Monoclinic	
Space group		$P2_1/m$	
a [Å]	4.4988(1)	4.5261(1)	4.3581(1)
b [Å]	10.3421(2)	10.3967(2)	10.2079(2)
c [Å]	6.7783(2)	6.8304(2)	7.1065(2)
β [°]	105.779(3)	105.755(3)	104.639(3)
Z		2	
Volume [Å^3]	303.49	309.34	305.88
Density, calc [g cm^{-3}]	6.16	6.98	6.17
Index ranges	$-7 < h < 7$	$-7 < h < 7$	$-6 < h < 7$
	$-16 < k < 16$	$-16 < k < 16$	$-16 < k < 16$
	$-10 < l < 10$	$-11 < l < 11$	$-11 < l < 11$
Reflections collected	12 198	13 835	14 297
Temperature [K]	290	290	290
Radiation		Mo Kα	
Unique data/parameters	1402/32	1414/32	1422/32
μ [mm^{-1}]	24.9	48.5	25.1
R_1/wR_2 ($I > 2\sigma(I)$)	0.0303/0.0655	0.0197/0.0448	0.0263/0.0630
R_1/wR_2 (all data)	0.0363/0.0705	0.0205/0.0450	0.0276/0.0635
GoF	1.142	1.162	1.178
Highest peak/hole [e$^-$ Å^{-3}]	3.77/−2.45	3.37/−2.08	3.73/−1.86
M—La bond lengths [Å]	3.2642(5)–3.4376(3)	3.3222(4)–3.4663(3)	3.2618(6)–3.4947(5)
C—C bond lengths [Å]	1.32(1)	1.332(8)	1.343(9)
La—C bond lengths [Å]	2.479(5)–2.908(5)	2.477(4)–2.913(4)	2.432(4)–2.833(4)

quoting the depository numbers CSD-2 427 328, 2 427 474, and 2 427 475.

Powder X-ray diffraction (PXRD) data were collected for La_3BiC_2 using a Rigaku SmartLab diffractometer (Cu Kα source, 40 kV, 44 mA). Crystals were ground to powder under inert atmosphere and placed in a zero-background sample holder. To prevent oxidation, a thin Kapton film was placed over the powder and affixed in place with apiezon grease. Data were collected from 20° to 80° 2-θ with a step size of 0.03° at 4 s per step.

2.4. Electronic Structure Calculations

DOS and crystal orbital Hamilton population (COHP) data for La_3TeC_2 and La_3BiC_2 were calculated using the Stuttgart TB–LMTO–ASA (tight binding–linear muffin tin orbital–atomic sphere approximation) software package.[17] The models were based on the space group, unit cell parameters, and atomic coordinates determined from single-crystal X-ray diffraction analyses. An 18 × 18 × 6 k-point grid was used in the integrations; this was processed using the tetrahedron method.[18] The orbital basis sets used for these calculations consisted of La (6*s*, 5*d*, 4*f*), C (2*s*, 2*p*), Te (5*s*, 5*p*, 4*d*), and Bi (6*s*, 6*p*, 5*d*, 4*f*), with La (6*p*), C (3*d*), Te (5*d*), and Bi (6*p*) being downfolded.

3. Results and Discussion

3.1. Synthesis

Many Ln/M/C compounds are known with *M* = group 13 and 14, but far fewer with group 15 or 16, and none with *M* = heavy pnictides and chalcogenides. This latter gap is likely due to the very different melting points and reactivities of *M* versus carbon. These elements also do not form binary phases with each other; graphite can be used as a crucible for reactions rich in these *M* elements. However, both *M* and carbon do form binary lanthanide compounds. Lanthanum (particularly in excess) can therefore be used as a bridging element to bring these elements together into one compound. This can be viewed as an example of bringing an "antagonistic pair" of elements (carbon and *M*) together using a third element (La) that segregates the immiscible atoms into spatially separated substructures.[19]

The La_3MC_2 compounds form as silver, rod-shaped crystals as shown in **Figure 1**. The crystal size and yield depend on M. The bismuth analog forms in highest yield (70%, based on amount of Bi reactant used) with the largest crystals (0.1 mm in width, 2 mm in length). The antimony and tellurium analogs form with lower yield (50% and 20%, respectively). Attempts to make a selenium analog from reaction of Se and C in La/Ni flux were not successful. Stoichiometric synthesis (combining La, M, and C elements in a 3:1:2 mole ratio) were also not successful, producing binary phases. All of the La_3MC_2 compounds are air sensitive and must be stored under argon, but they can be handled briefly in air. They dissolve readily in water, with vigorous evolution of gas as seen in Figure 1 (likely due to reaction of the C_2^{4-} units to form ethylene).

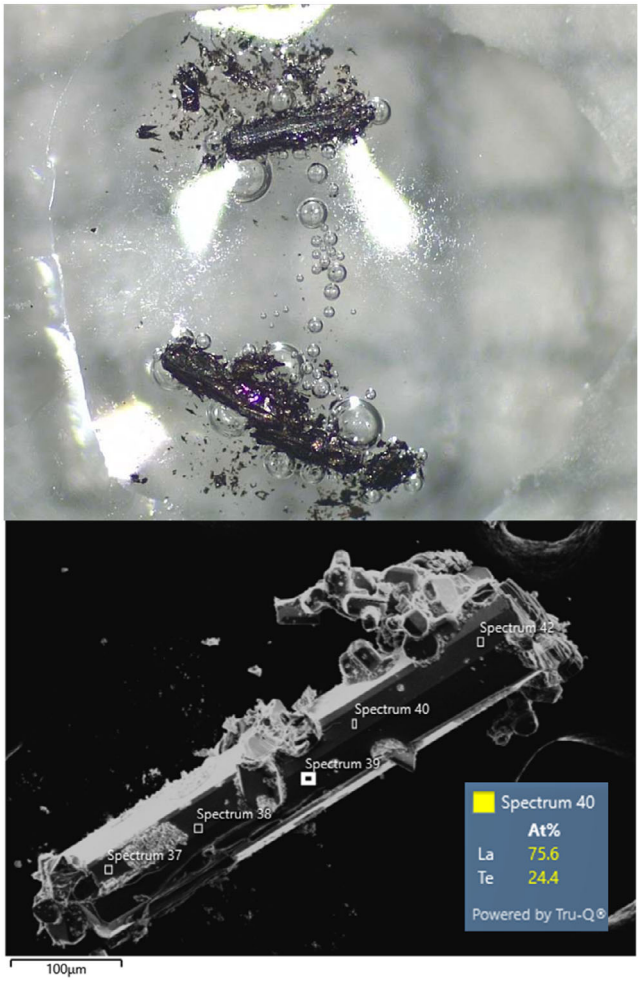

Figure 1. *Top:* Microscope image on mm grid paper of crystals of La_3BiC_2 reacting in a drop of water. *Bottom:* Scanning electron microscope image of a crystal of La_3TeC_2, along with SEM–EDS elemental analysis.

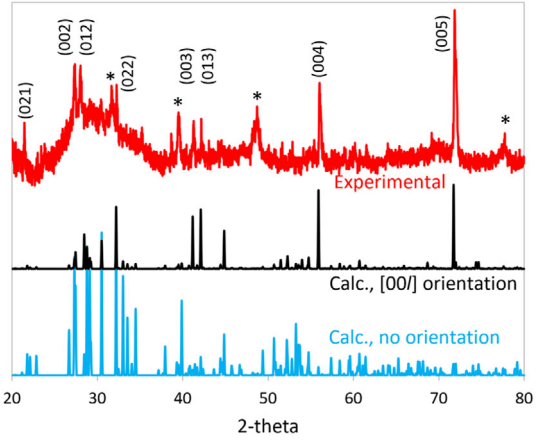

Figure 2. Powder X-ray diffraction pattern of La_3BiC_2 (red), compared to calculated patterns based on the crystal structure. The bottom pattern (blue) assumes no preferred orientation; the middle pattern is calculated with preferred orientation in the [00l] direction. Impurity peaks due to lanthanum residue and byproducts are marked with asterisks.

PXRD data were collected for La_3BiC_2; the resulting pattern is shown in **Figure 2**. The data are compared to theoretical PXRD patterns based on the structure determined from single-crystal diffraction studies (see next section), either calculated with no preferred orientation, or with partial alignment along the [00*l*] direction. The experimental pattern clearly exhibits a strong preferred orientation, as seen by the increased intensity of the (00*l*) peaks. There are also additional broad peaks due to lanthanum metal residue from the flux that adheres to the products.

3.2. Structure

The structure of the La_3MC_2 compounds features M^{n-} and C_2^{x-} anions surrounded by lanthanide cations. **Figure 3** shows the overall structure viewed down the *a* axis and the coordination environments of the anions. The large main group anions (Sb, Bi, or Te) are coordinated by 8 La^{3+} cations with bond lengths ranging from 3.2618(6)–3.4947(5) Å (Table 1). These are similar to the range of bond lengths seen in binary La/M compounds such as NaCl-type LaSb, LaBi, and LaTe (3.245, 3.29, and 3.218 Å respectively), La_5Bi_3 (3.38 Å), and $LaTe_2$ (3.269 Å).[20–22] The carbide anion is found in an octahedral coordination, with a similar C—C bond length for all three La_3MC_2 analogs, in the 1.32–1.34 Å range. This indicates a double bond, similar to a C_2^{4-} ethylene anion, as is found in $La_5Ge_2C_2$.[23] The orthorhombic structure of $La_5Ge_2C_2$ also features a network of face-sharing M@La_n polyhedra with C_2 units in octahedral interstitial sites, although in that case the Ge anions are surrounded by 9 La cations instead of 8

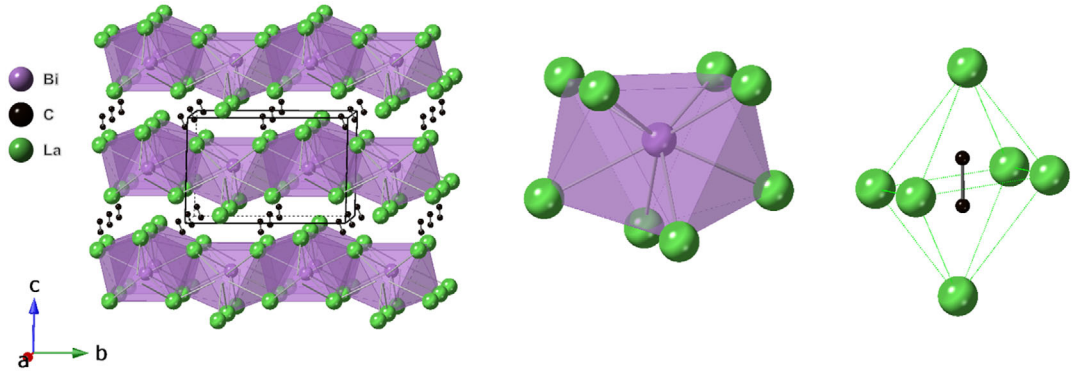

Figure 3. Structure of La_3BiC_2, with the environment of bismuth atoms shown in polyhedral mode. The distorted octahedral environment of the C_2 unit is also highlighted.

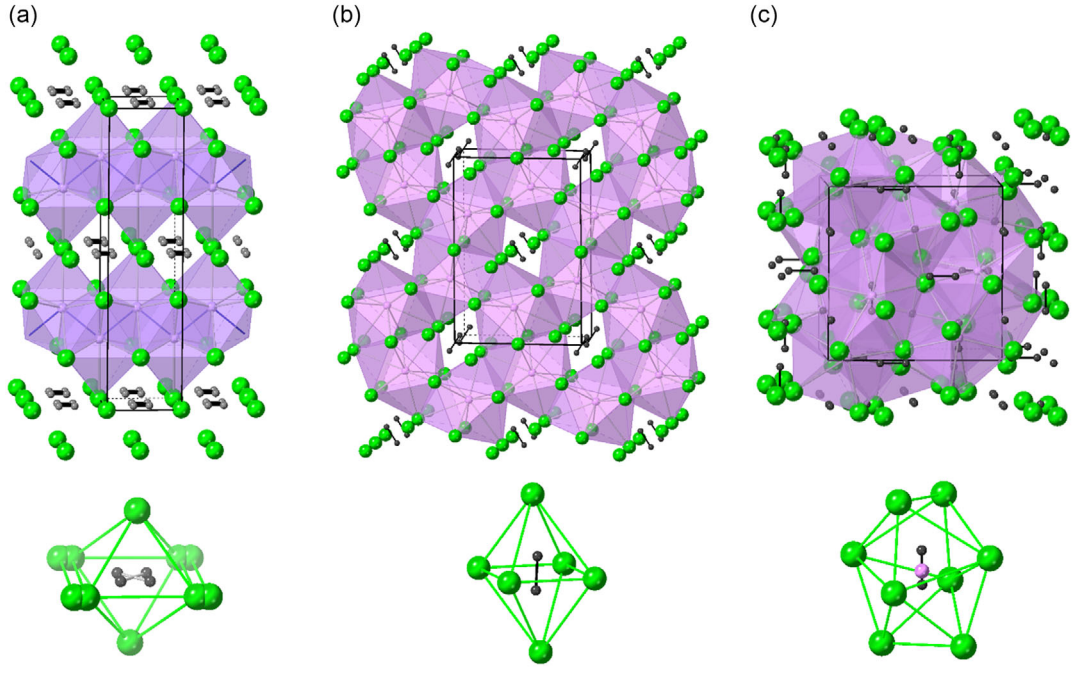

Figure 4. The structures of other La/M/C ternary compounds with C_2 units. Lanthanum atoms are green spheres, and carbon shown as small black spheres. Main group atoms (M = Si, Ge, P) shown as purple polyhedra: a) $La_3Si_2C_2$, b) $La_5Ge_2C_2$, and c) $La_4(P/C_2)_3$.

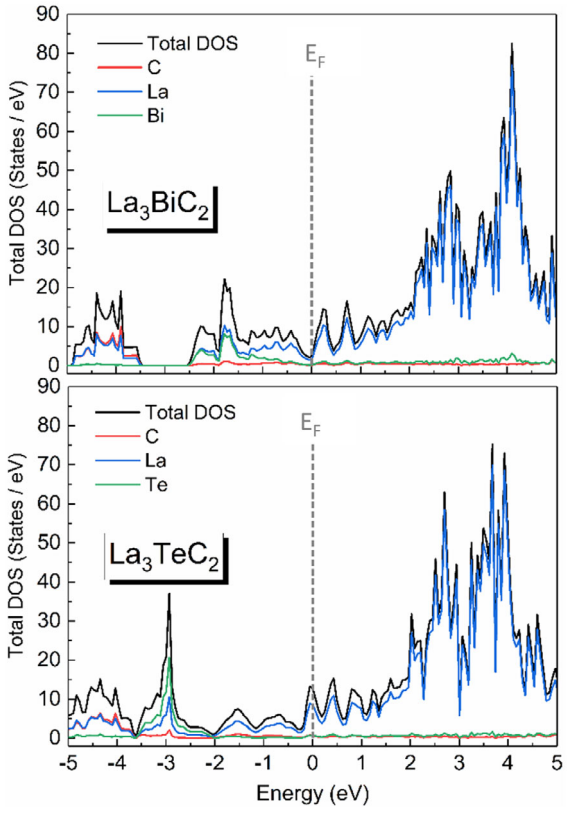

Figure 5. Density of states data for La_3BiC_2 and La_3TeC_2. The Fermi level is set to 0 eV.

(see **Figure 4**). It is notable that the orbitals of the C_2 units in these compounds do interact with the lanthanide matrix, so a simplistic view of these species as C_2^{4-} is not valid. An investigation of the structure and bonding of superconducting LaC_2, which also contains C_2 units in octahedral coordination (with a C—C bond length of 1.294(2) Å), indicated hybridization between the carbon *p*-orbitals and lanthanum d-states.[24] Comparison with the C—C bonds in other lanthanum carbides and lanthanum carbide halides indicated a potential correlation between bond length and superconducting temperature, with T_c maximized for C—C bond lengths around 1.30 Å.

Many of the previously reported Ln/M/C phases with main group elements can be viewed as interstitial carbides, with monatomic carbon atoms partially occupying octahedral interstitial sites. These include Ln_3MC_x (M = Al, Ga, In, Tl, Sn) with the stuffed Cu_3Au structure (or perovskite structure, if $x = 1$), and $Ln_5M_3C_x$ (M = Si, Ge, Sn) with Cr_5Si_3B-related structures.[12] Both of these classes of materials have variable occupancy of the carbon, while the M atoms are ordered and coordinated by 9 or 12 Ln cations. Other Ln/M/C phases contain C_2 units similar to those found in the La_3MC_2 structure; these are shown in Figure 4. $Ln_3Si_2C_2$ compounds contain zig-zag chains of silicon and C_2 units disordered in octahedral sites.[25] $La_4(P/C_2)_3$ and $La_4Ge(C_2)_2$ are essentially substitutional variants of La_2C_3.[26,27] This is more accurately written as $La_4(C_2)_3$, to represent the presence of C_2 units in eightfold coordination by La cations. In the ternary variants, the germanium or phosphorus anions mix on the C_2 site. Of all the reported Ln/M/C compounds, $La_5Ge_2C_2$ bears the strongest resemblance to the La_3MC_2 title

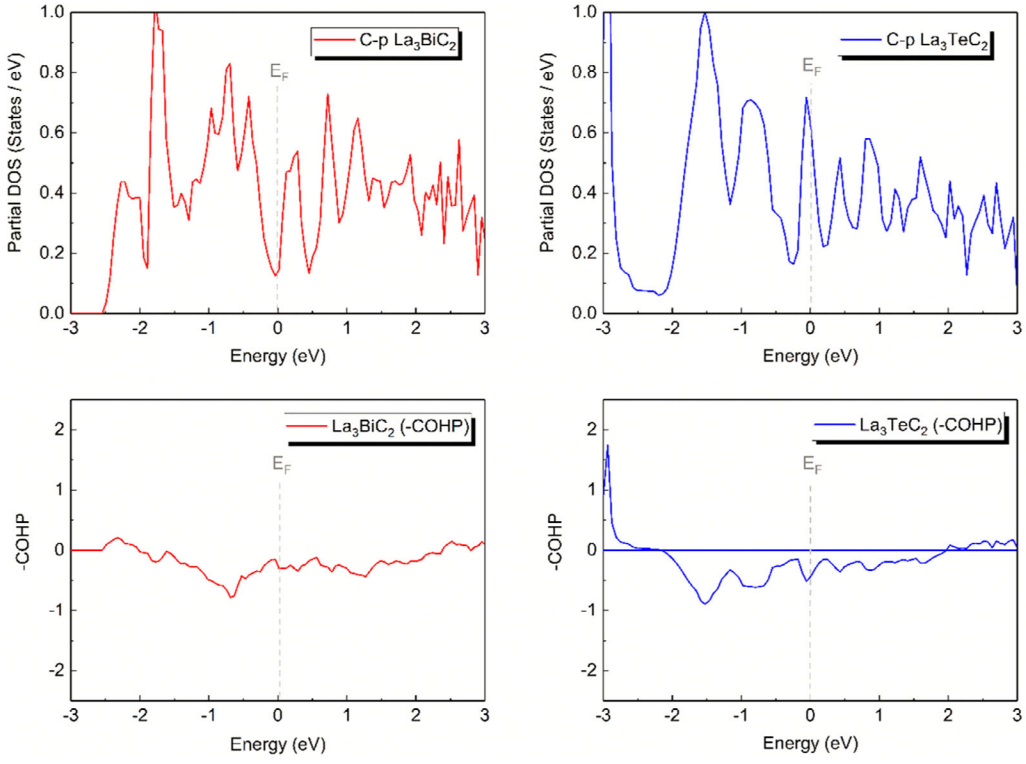

Figure 6. The partial density of states (DOS) and crystal orbital Hamilton population (COHP) data for the carbon *p*-states for La_3BiC_2 and La_3TeC_2. The Fermi level is set to 0 eV.

compounds in that it contains a main group *M* element coordinated by 8–9 La cations, while the C_2 units are in octahedral sites.

3.3. Electronic Structure

Despite the presence of La^{3+} cations, and anions recognizable as C_2^{4-} and $Bi^{3-}/Sb^{3-}/Te^{2-}$, these La_3MC_2 compounds are not charge-balanced. This places these materials between the saltlike carbides such as $La_2C_2Br_2$ and the metallic compounds $La_5C_2Ge_2$. Electronic structure calculations were carried out on La_3MC_2 compounds to further explore this; the DOS diagrams are shown in **Figure 5**. The Fermi level of the bismuth analog is positioned in a pseudogap, indicating that the compound is a poor metal. The bismuth states are predominantly located in the −3 to 0 eV region, in agreement with the anionic nature of this element. Similarly, carbon *s*-states are present in a narrow band between −4 and −5 eV. The empty valence orbitals of lanthanum contribute to the bands above E_F. Replacement of bismuth with tellurium adds one more electron to the system; this shifts the Fermi level into a small peak in the DOS, indicating that La_3TeC_2 should be a more metallic compound. This also suggests that the number of carriers and associated properties may be tunable by making a solid solution $La_3(Bi_xTe_{1-x})C_2$. The tellurium states of La_3TeC_2 are found in the −2 to −4 eV region, a narrower and more stabilized anion band compared to the bismuth states in La_3BiC_2, in accordance with the smaller size and higher electronegativity of Te.

While the electronic properties of the La_3MC_2 compounds have not yet been measured, it is of interest to compare the behavior of the carbide states near the Fermi level to that seen in related materials that also feature C_2 units. The partial density of the *p*-orbitals of carbon near E_F is highlighted in **Figure 6**. In both La_3BiC_2 and La_3TeC_2 these carbon orbitals are hybridizing with lanthanum *d*-orbitals that make the predominant contribution to the states near the Fermi level (see Figure 5), similar to the behavior reported for LaC_2.[24] The bismuth analog shows narrow peaks just above and below the Fermi level, resulting in a pseudogap at E_F. This is similar to what was reported for the carbon π^* states in $Y_2C_2I_2$; the hybridization of these states with the broader band derived from the *d*-orbitals of Y is thought to be crucial to the superconductivity of that compound.[9,28] The similar features seen for La_3BiC_2 and the fact that the location of the Fermi level

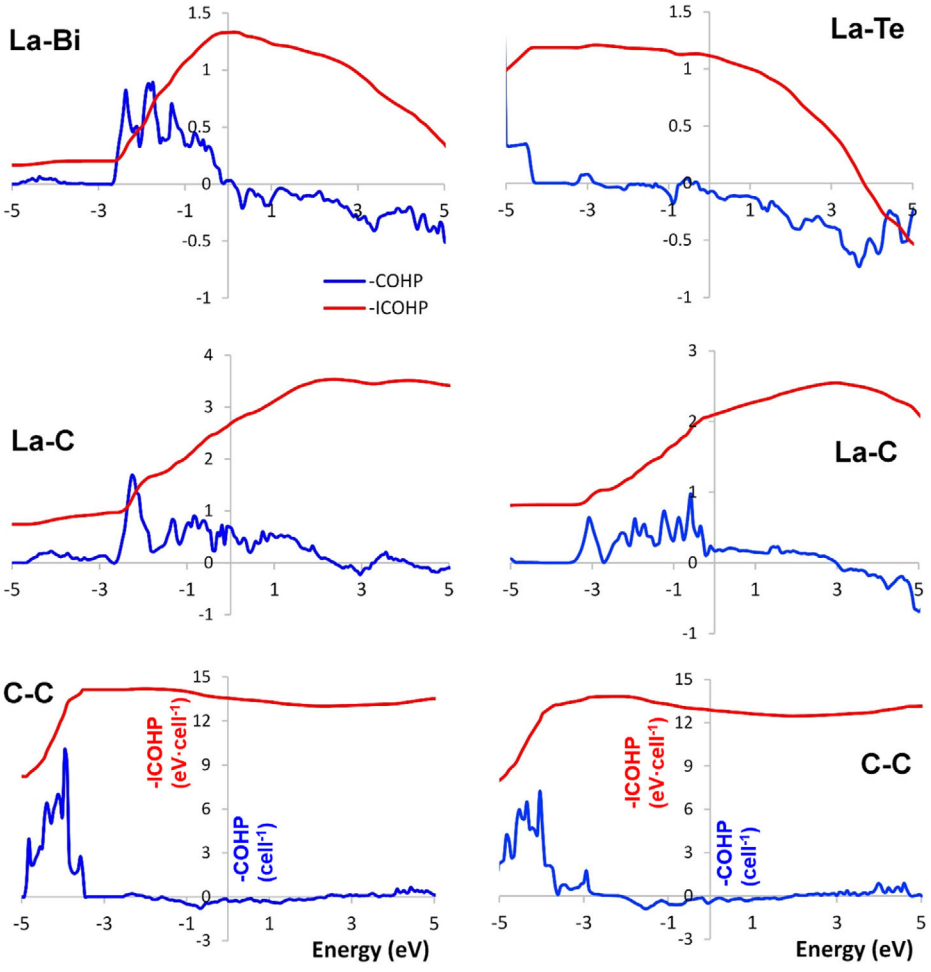

Figure 7. Crystal orbital Hamilton population (COHP; in blue) and integrated COHP (iCOHP; in red) data for selected interactions in La_3BiC_2 (left) and La_3TeC_2 (right). The Fermi level is positioned at 0 eV.

with respect to the pseudogap can be shifted by substituting Te for Bi is promising for potentially tuning the electronic behavior of this system.

Further information about the nature of these compounds was sought by carrying out COHP calculations to explore the interactions between specific atoms in the structure. Data for the C—C orbital interactions near E_F for both La_3BiC_2 and La_3TeC_2 are shown in **Figure** 6 and **7**. The C—C states near the Fermi level appear to be predominantly antibonding, confirmed by the decreasing integrated-COHP (iCHOP) values at E_F for the C—C bond in Figure 7, indicating these are likely π^* orbitals of the C_2 unit that are partially filled. The similar behavior in both analogs is in agreement with the observed similar C—C bond lengths. The La—C interactions are also similar for both La_3MC_2 compounds, with bonding states at the Fermi level. It is notable that this iCOHP is maximized for both compounds above E_F, indicating that addition of more electrons would strengthen the La—C bonding. This concurs with the electron-poor compositions of $(La^{3+})_3Bi^{3-}(C_2)^{4-}$ and $(La^{3+})_3Te^{2-}C_2)^{4-}$, which would achieve charge-balance if more electrons were added. However, the interaction between the heavy metal *M* and surrounding lanthanum cations is optimized for the *M*═Bi analog, with bonding states occupied below E_F and antibonding states empty; this maximizes the La—Bi iCOHP. Conversely, the data for La_3TeC_2 show antibonding states at the Fermi level and a decreasing iCOHP.

4. Conclusion

The isolation of new La_3MC_2 compounds from reactions in La-rich melts demonstrates the usefulness of the metal flux synthesis method to bring highly disparate elements into solution and enable formation of multinary compounds instead of simple binary phases. These materials represent a new family of lanthanide carbide materials containing layers of C_2 anions in octahedral coordination by lanthanum cations, separated by layers of *M* anions. The formation of analogs with M = Sb, Bi, and Te indicates that the valence electron count of these materials can be tuned, potentially enabling doping into a superconducting state in a substitutional variant such as $La_3(Bi_{1-x}Te_x)C_2$.

Acknowledgements

This project was supported by the National Science Foundation Division of Materials Research (grant no. DMR-2126077). This work made use of the X-ray Characterization Center in the FSU Department of Chemistry and Biochemistry (grant no. FSU075000XRAY).

Conflict of Interest

The authors declare no conflict of interest.

Data Availability Statement

The data that support the findings of this study are openly available in [Fachinformationzentrum Karlsruhe] at [https://icsd.products.fiz-karlsruhe.de/], reference number [2427475].

Keywords: carbides · crystal growths · intermetallic phases · lanthanides · X-ray diffraction

[1] E. Dashjav, G. Kreiner, W. Schnelle, F. R. Wagner, R. Kniep, W. Jeitschko, *J. Solid State Chem.* **2007**, *180*, 636.
[2] F. R. Deboer, Y. K. Huang, Z. D. Zhang, D. B. Demooij, K. H. J. Buschow, *J. Mag. Magn. Mater.* **1988**, *72*, 167.
[3] J. M. D. Coey, S. Hong, Y. Otani, D. P. F. Hurley, *J. Mag. Magn. Mater.* **1991**, *98*, 76.
[4] J. Zaikina, H. Zhou, S. Latturner, *J. Solid State Chem.* **2010**, *183*, 2987.
[5] A. S. Jayasinghe, S. E. Latturner, *Cryst. Growth Des.* **2021**, *21*, 103.
[6] A. Simon, H. Mattausch, R. Eger, R. K. Kremer, *Angew. Chem. Int. Ed.* **1991**, *30*, 1188.
[7] M. Backer, A. Simon, R. K. Kremer, H. J. Mattausch, R. Dronskowski, J. Rouxel, *Angew. Chem. Int. Ed.* **1996**, *35*, 752.
[8] G. J. Miller, *The Chemistry of Transition Metal Carbides and Nitrides*, (Ed: S. T. Oyema), Chapman & Hall, London **1996**, pp. 134–153.
[9] R. K. Kremer, J. S. Kim, A. Simon, *High Tc Superconductors and Related Transition Metal Oxides*, (Eds: A. Bussmann-Holder, H. Keller), Springer-Verlag, Berlin Heidelberg **2007**, pp. 213–226.
[10] V. Babizhetskyy, B. Kotur, V. Levytskyy, H. Michor, *Handbook on the Physics and Chemistry of Rare Earths*, Elsevier, Amsterdam, New York **2017**, Vol. *52*, pp. 1–263.
[11] G.-Y. Adachi, N. Imanaka, F. Zhang, *Handbook on the Physics and Chemistry of Rare Earths*, Vol. *15*, Elsevier, Amsterdam, New York **1991**, pp. 61–189.
[12] S. E. Latturner, *Handbook on the Physics and Chemistry of Rare Earths*, Vol. *65*, Elsevier, Amsterdam, New York **2024**, pp. 275–319.
[13] M. G. Kanatzidis, R. Pöttgen, W. Jeitschko, *Angew. Chem. Int. Ed.* **2005**, *44*, 6996.
[14] E. M. Benbow, N. S. Dalal, S. E. Latturner, *J. Am. Chem. Soc.* **2009**, *131*, 3349.
[15] CrysAlisPRO, Oxford Diffraction/Agilent Technologies UK Ltd, Yarnton, England **2014**.
[16] C. B. Hubschle, G. M. Sheldrick, B. Dittrich, *J. Appl. Crystallog.* **2011**, *44*, 1281.
[17] O. K. Andersen, T. Saha-Dasgupta, R. W. Tank, C. Arcangeli, O. Jepsen, G. Krier, *Electronic Structure and Physical Properties of Solids. The Uses of the LMTO Method*, (Ed: H. Dreyssé), Springer, Berlin **2000**, pp. 3–84.
[18] P. E. Blöchl, O. Jepsen, O. K. Andersen, *Phys. Rev. B* **1994**, *49*, 16223.
[19] T. J. Slade, N. Furukawa, M. Dygert, S. Mohamed, A. Das, W. Xia, C. Z. Wang, S. L. Bud'ko, P. C. Canfield, *Phys. Rev. Mater.* **2024**, *8*, 064401.
[20] K. Yoshihara, J. B. Taylor, L. D. Calvert, J. G. Despault, *J. Less-Common Met.* **1975**, *41*, 29.
[21] A. A. Eliseev, E. I. Yarembash, V. G. Kuznetsov, L. I. Antonova, Z. P. Stoyantsova, *Inorg. Mater.* **1965**, *1*, 943.
[22] G. V. Samsonov, M. N. Abdusalyamova, K. Shokirov, S. A. Pryakhina, *Inorg. Mater.* **1974**, *10*, 1672.
[23] W. Carrillo-Cabrera, J. Curda, K. Peters, M. Kohout, H. G. von Schnering, *Z. Anorg. Allg. Chem.* **2004**, *630*, 2186.

[24] V. Babizhetskyy, O. Jepsen, R. K. Kremer, A. Simon, B. Ouladdiaf, A. Stolovits, *J. Phys.: Condens. Matter* **2014**, *26*, 025701.
[25] W. Jeitschko, M. H. Gerdes, A. M. Witte, U. C. Rodewald, *J. Solid State Chem.* **2001**, *156*, 1.
[26] W. Carrillo-Cabrera, J. Curda, K. Peters, H. G. von Schnering, *J. Solid State Chem.* **1999**, *147*, 372.
[27] P. S. Chizhov, W. Schnelle, U. Burkhardt, M. Schmidt, Y. Prots, E. V. Antipov, Y. Grin, *Z. Anorg. Allg. Chem.* **2010**, *636*, 1318.
[28] P. Puschnig, C. Ambrosch-Draxl, R. W. Henn, A. Simon, *Phys. Rev. B* **2001**, *64*, 024519.

Manuscript received: February 28, 2025
Revised manuscript received: May 13, 2025
Version of record online: